
The SuperCDMS Experiment

R.W. Schnee¹, D.S. Akerib¹, M.J. Attisha², C.N. Bailey¹, L. Baudis³,
 D.A. Bauer⁴, P.L. Brink⁵, P.P. Brusov¹, R. Bunker⁶, B. Cabrera⁵,
 D.O. Caldwell⁶, C.L. Chang⁵, J. Cooley⁵, M.B. Crisler⁴, P. Cushman⁷,
 P. Denes⁸, M.R. Dragowsky¹, L. Duong⁷, J. Filippini⁹, R.J. Gaitskell²,
 S.R. Golwala¹⁰, D.R. Grant¹, R. Hennings-Yeomans¹, D. Holmgren⁴,
 M.E. Huber¹¹, K. Irwin¹², A. Lu⁸, R. Mahapatra⁶, P. Meunier⁹,
 N. Mirabolfathi⁹, H. Nelson⁶, R.W. Ogburn⁵, E. Ramberg⁴, A. Reisetter⁷,
 T. Saab³, B. Sadoulet^{9,8}, J. Sander⁶, D.N. Seitz⁹, B. Serfass⁹,
 K.M. Sundqvist⁹, J-P.F. Thompson², S. Yellin⁶, J. Yoo⁴, and B.A. Young¹³

¹ Department of Physics, Case Western Reserve University, Cleveland, OH 44106, USA schnee@case.edu

² Department of Physics, Brown University, Providence, RI 02912, USA

³ Department of Physics, University of Florida, Gainesville, FL 32611, USA

⁴ Fermi National Accelerator Laboratory, Batavia, IL 60510, USA

⁵ Department of Physics, Stanford University, Stanford, CA 94305, USA

⁶ Department of Physics, University of California, Santa Barbara, CA 93106, USA

⁷ School of Physics & Astronomy, University of Minnesota, Minneapolis, MN 55455, USA

⁸ Lawrence Berkeley National Laboratory, Berkeley, CA 94720, USA

⁹ Department of Physics, University of California, Berkeley, CA 94720, USA

¹⁰ California Institute of Technology, Pasadena, CA, 91125, USA

¹¹ Department of Physics, University of Colorado at Denver and Health Sciences Center, Denver, CO 80217, USA

¹² National Institute of Standards and Technology, Boulder, CO 80303, USA

¹³ Department of Physics, Santa Clara University, Santa Clara, CA 95053, USA

1 Introduction

Nonluminous, nonbaryonic, weakly interacting massive particles (WIMPs) [1, 2] may constitute most of the matter in the universe [3]. WIMPs are expected to be in a roughly isothermal Galactic halo. They would interact elastically with nuclei, generating a recoil energy of a few tens of keV, at a rate $\lesssim 1$ event $\text{kg}^{-1} \text{d}^{-1}$ [2, 4, 5].

Supersymmetry provides a natural WIMP candidate in the form of the lightest superpartner [5]. Figure 1 shows the WIMP masses and cross sections that are consistent with the three primary approaches to supersymmetry. Regardless of the theoretical philosophy, sensitivity from elastic-scattering exper-

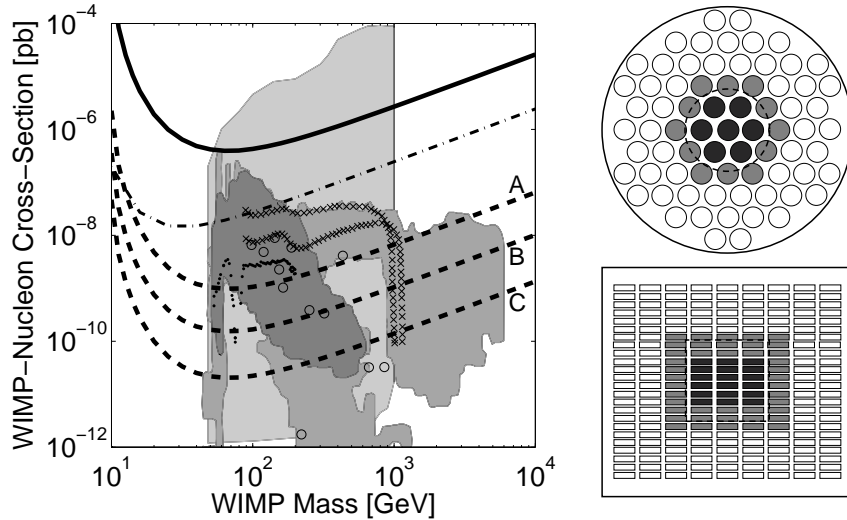


Fig. 1. *Left:* Reach of SuperCDMS phases A, B, and C (dashed curves) with current CDMS II limit [6] (solid curve) and sensitivity goal (dot-dashed curve). The lightest grey region results from a scan of MSSM parameter space [7]. SuperCDMS will probe nearly all split-supersymmetry models (\times 's [8] and dots [9]) and much of the mSUGRA region [10] (medium grey), including most post-LEP benchmark points (circles) [11] and nearly all the subset (dark grey) consistent with a supersymmetric interpretation of the muon $g - 2$ measurement. *Right:* Top view (above side view) of SuperCDMS cryostat showing deployment of 7 towers of 6 detectors each in 25-kg phase A (darkest circles), 19 towers of 12 detectors each in 150-kg phase B (grey circles), and 73 towers of 24 detectors each in 1-ton phase C (all circles). The cryostat will be $3\times$ larger than the CDMS cryostat (dashes) in each dimension.

iments to WIMP-nucleon scalar cross-sections in the range 10^{-46} – 10^{-44} cm^2 would be of great interest.

To probe to such small cross sections, it helps to operate without backgrounds, so that the search sensitivity is directly proportional to the detector mass \times exposure time (MT). Under subtraction of an estimated background, the sensitivity becomes proportional to \sqrt{MT} . Ultimately, the subtraction becomes limited by systematics, preventing further improvement in sensitivity. CDMS ZIP detectors [12] have excellent background rejection, making them the most proven means by which to operate an experiment without backgrounds.

CDMS ZIP detectors allow discrimination between WIMP nuclear recoils and background electron recoils through two effects. First, for a given energy, recoiling electrons are more ionizing than recoiling nuclei, resulting in a higher ratio of ionization to phonon signal, called “ionization yield.” Second, the athermal phonon signals due to nuclear recoils have longer rise times and

occur later than those due to electron recoils. For recoils within a few μm of a detector’s surface (primarily from low-energy electrons), the charge collection is incomplete [13], making discrimination based on ionization yield less effective. But these events can be effectively rejected by phonon timing cuts because they have, on the average, even faster phonon signals than those from bulk electron recoils [14, 15].

In order to probe to smaller WIMP-nucleon cross sections, we plan to increase the detector mass of the experiment in several phases, resulting in a ton-scale SuperCDMS experiment (previously called CryoArray [16, 17]). To maximize the discovery potential of the experiment, each phase will have an expected background smaller than one event. The excellent characterization of backgrounds and the information from ZIP detectors on each event would minimize the ambiguity of a discovery. The low energy thresholds and small “quenching” factors for both the ionization and the phonon measurements allow the requirement of a positive signal for both energy measurements, providing immunity to artifacts that may mimic a WIMP signal. The $\sim\text{keV}$ energy resolutions and $\sim\text{mm}$ position resolution would allow detailed tests of consistency with a WIMP signal. A test for annual modulation would depend only on accurately knowing the efficiency for WIMPs over time, since there would be no additional backgrounds.

To keep backgrounds negligible during the phases of SuperCDMS, improvements are needed in the level and discrimination of backgrounds, described in Sections 2 and 3 respectively. To achieve an exposure of 500 ton d within a reasonable time and budget, manufacturability and detector production rates must be improved, as discussed in Section 4.

2 Reduction of Backgrounds

2.1 Neutrons

A neutron of kinetic energy $\sim 2\text{ MeV}$ can cause a recoil that is indistinguishable from one caused by a WIMP. Polyethylene shielding and an active scintillator veto are used to minimize or reject the neutron background. For the CDMSII experiment at the Soudan Mine, most neutrons that cause unvetoes nuclear recoils in Ge come from the $\sim 220\text{ GeV}$ muons that penetrate to and interact in the rock surrounding the CDMSII experimental hall. Simulations indicate the rate of unvetoes neutron-induced recoils from showers in the rock at Soudan is $3 \times 10^{-4}\text{ kg}^{-1}\text{ d}^{-1}$, sufficiently low that it should be important only for exposures significantly larger than those planned for CDMSII (1000 kg d). To reduce this background for the $10\times$ to $500\times$ larger exposures of SuperCDMS, we plan to build the experiment at SNOLab, where the increased depth suppresses the dominant neutron backgrounds by over two orders of magnitude compared to Soudan.

Table 1. Mean event rates between 15–45 keV recoil energy in the inner Ge detectors of CDMSII and SuperCDMS, per 500 ton day exposure. CDMSII photon (γ) and electron (β) rates of events with full ionization yield (“Bulk”) and reduced ionization yield (“Surface”) are inferred from calibrations, simulations, and measurements. Leakage into the nuclear-recoil signal region with phonon-timing cuts applied is based on calibrations.

	CDMS II						SuperCDMS		
	Bulk		Surface		Leakage		Improve	Leakage	
	all	singles	all	singles	wo/cuts	w/cuts	Clean	Reject	Goal
All	6×10^7	1.5×10^7	600000	170000	20000	600	2×	100×	< 1.0
γ	6×10^7	1.5×10^7	350000	100000	2500	70	2×	100×	< 0.5
β	7×10^9	2×10^9	250000	70000	17000	500	10×	100×	< 0.5

2.2 Electron and Photon Backgrounds

CDMS ZIP discrimination of electron-recoil events based on ionization yield is essentially perfect for electrons or photons interacting in the bulk of the detector. However, events within $\sim 35 \mu\text{m}$ of the detector surface suffer ionization-yield suppression, and events in the first $\sim 1 \mu\text{m}$ lose so much ionization that they may be misidentified as nuclear recoils. Phonon timing provides rejection of 97% of these “surface events” while keeping 70% of true nuclear recoils.

Rejection of photon-related backgrounds in the CDMSII experiment has been measured using high-energy photon sources. Rejection of photon and electron backgrounds has been simulated using GEANT4, including tracking of low-energy electrons created by photon interactions and inferred depth-dependent ionization yield based on calibrations with an electron source [15]. The simulations and measurements both indicate that of all photon-related events (15-45 keV), 0.3% are single-scatter surface events with some ionization-yield suppression, and 1.8% of those (or 0.005% of all photon-related events) suffer enough ionization-yield suppression to be misidentified as nuclear recoils (see Table 1). Thus, rejection is 99.995% efficient based on the number of scatters and ionization yield alone, and is 99.9999% after applying the phonon-timing cut.

Table 1 shows that the background of surface singles is about twice as large as the inferred contribution from photon-related events, implying that about half the surface singles are due to surface radioactive beta contaminants. As shown in Fig. 2, surface betas cause very shallow interactions and thus suffer far higher misidentification than photon-induced events, resulting in background leakage $\sim 7\times$ worse than that due to photons.

Background-reduction efforts will therefore center on reducing the surface beta contamination by a factor of 10 by identifying the contaminants and changing fabrication procedures to prevent their introduction. Table 2 lists screening methods for 79 beta-emitting and electron-capture isotopes. Inductively-coupled-plasma mass spectrometry (ICP-MS) would provide the quickest screening method for isotopes for which its sensitivity (typically 1 ppb

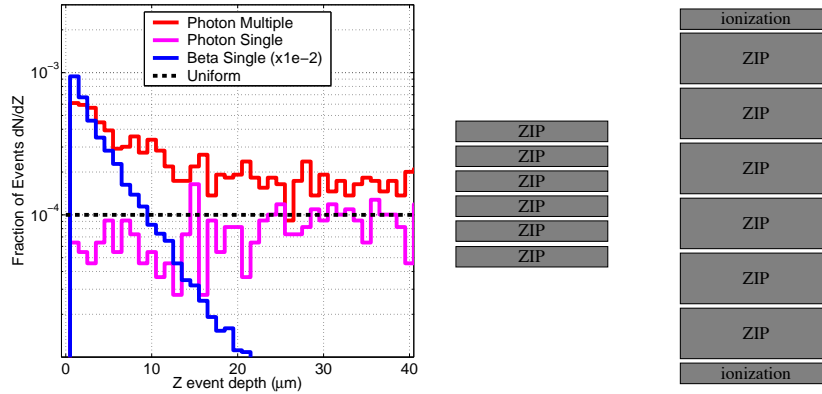


Fig. 2. Number of simulated events as a function of depth (left). Single-scatter photon-induced events (lower grey) are uniformly distributed in depth, and multiple-scatter events (upper grey) are biased toward the surface. Events from a beta emitter (black) show a steep falloff with depth, making them the most dangerous. Side views show a stack of cylindrical SuperCDMS ZIP detectors (right) will be 2.5× thicker than CDMS ZIPs (center), with ionization endcap detectors to reduce or veto electrons incident on the outermost ZIP surfaces.

Table 2. Detection schemes for all long-lived beta-emitting isotopes. Isotopes in boldface may be detected by ICP-MS with sensitivity between 1 ppb and 1 ppt.

Method	Applicable Isotopes
ICP-MS (1 ppb)	^{40}K ^{48}Ca ^{50}V ^{87}Rb ^{92}Nb ^{98}Tc ^{113}Cd ^{115}In ^{123}Te ^{138}La ^{176}Lu ^{182}Hf ^{232}Th ^{235}U ^{238}U ^{236}Np ^{250}Cm
ICP-MS (1 ppt)	^{10}Be ^{36}Cl ^{60}Fe ^{79}Se ^{93}Zr ^{94}Nb ^{97}Tc ^{99}Tc ^{107}Pd ^{126}Sn ^{129}I ^{135}Cs ^{137}La ^{154}Eu ^{158}Tb ^{166m}Ho ^{208}Bi ^{208}Po ^{209}Po ^{252}Es
γ	^{40}K ^{50}V ^{60}Fe ^{60}Co ^{93}Zr ^{92}Nb ^{94}Nb ^{93}Mo ^{98}Tc ^{99}Tc ^{101}Rh ^{101m}Rh ^{102m}Rh ^{109}Cd ^{121m}Sn ^{126}Sn ^{125}Sb ^{129}I ^{134}Cs ^{137}Cs ^{133}Ba ^{138}La ^{145}Pm ^{146}Pm ^{150}Eu ^{152}Eu ^{154}Eu ^{155}Eu ^{157}Tb ^{158}Tb ^{166m}Ho ^{173}Lu ^{174}Lu ^{176}Lu ^{172}Hf ^{179}Ta ^{207}Bi ^{208}Bi ^{232}Th ^{235}U ^{238}U ^{236}Np ^{241}Pu
α	^{210}Pb ^{208}Po ^{209}Po ^{228}Ra ^{227}Ac ^{232}Th ^{235}U ^{238}U ^{236}Np ^{241}Pu ^{250}Cm ^{252}Es
β only	^3H ^{14}C ^{32}Si ^{63}Ni ^{90}Sr ^{106}Ru ^{113m}Cd ^{147}Pm ^{151}Sm ^{171}Tm ^{194}Os ^{204}Tl ^{10}Be ^{36}Cl ^{79}Se ^{97}Tc ^{107}Pd ^{135}Cs ^{137}La ^{154}Eu ^{209}Po

to 1 ppt) is good enough. A dozen isotopes including ^{210}Pb , a crucial background candidate, can be detected by their alpha emissions. An additional 25 isotopes may be detected by low-level γ -counting.

Finally, there are 12 to 21 isotopes, depending on ICP-MS sensitivity, that cannot be screened in any manner except by their emission of beta electrons. To detect these isotopes, we will develop a chamber capable of directly de-

tecting betas emitted from surfaces. This chamber will also serve as a very low-background α screener.

Further reductions in surface backgrounds will be achieved by decreasing the exposed surface area per detector mass, as shown in Fig 2. The major thrust in detector development will be in scaling up the detector thickness from 1 cm to 2.5 cm. The thicker detectors will have a $2.5\times$ smaller surface-to-volume ratio, thereby decreasing the background surface events per WIMP interaction by the same factor regardless of source. This increase requires new fabrication equipment and modifications to some of our present equipment. A larger voltage would be applied across these thicker detectors during their operation, resulting in only a slightly smaller drift field that would not significantly reduce the ionization yield for surface events.

Ge ionization detectors will act as an active veto shield around, above, and below the ZIP detectors. Ionization detectors cost ~ 5 times less to fabricate and test than the ZIPs. These veto detectors may reduce the contamination adjacent to the ZIPs; the CDMSI experiment indicated that the Ge detector material itself has the cleanest surfaces within the detector housings. Moreover, these detectors would reject the otherwise outermost ZIP detectors' dominant background of single-detector surface events caused by photons ejecting electrons from adjacent passive materials.

3 Detector Performance Improvements

The complementary method to reduce surface-event backgrounds in Super-CDMS is to improve the detector rejection of surface events. Improved analysis already is showing significant advances and should increase rejection by at least an order of magnitude. Further improvements can be achieved by optimization of both the charge collection and the athermal phonon sensors.

First, it is likely that we can improve the charge collection for surface events by optimizing the deposition of the amorphous-silicon layer used to prevent back-diffusion of carriers to the “wrong” electrode [13]. Older CDMS detectors with a different amorphous-silicon layer had a higher ionization yield for surface events than current detectors, resulting in $> 95\%$ rejection of surface betas based on ionization yield alone[18]. Returning to and possibly improving upon the old recipe should increase the blocking effectiveness of the electrodes against surface-event charge back-diffusion.

A longer-term goal is to enhance the information in the athermal phonon signals. Reading the phonon signal from the detector substrate faster should improve the pulse discrimination. The present ZIP detectors' phonon sensors cover only 20% of one surface of the detector substrate. New phonon-readout schemes described in Sect. 4 would allow increased surface-area coverage.

The most dramatic improvement in phonon read-out would occur if *both* sides of the disc-like detectors were instrumented with phonon sensors. This

double-sided readout should improve the phonon timing information by detecting the leading phonons on both faces of the detector. This design will symmetrize the detector response and allow a direct determination of the three-dimensional position of each event. The expected timing resolution of $0.5 \mu\text{s}$ at 10 keV would yield a position resolution of 1.5 mm in three dimensions.

One method of implementing this scheme keeps the same drift-field configuration used in the existing ZIP detectors. The problem then is to provide a voltage bias of up to $1 \mu\text{V}$ for the phonon sensors without adding more than a few picofarads to the capacitance of the ionization electrode, thereby degrading the ionization resolution. The best option is a high-frequency (20 MHz) AC power supply feeding a small transformer. A diode and LC filter on the secondary produce the appropriate bias. The voltage applied could be regulated at low bandwidth by monitoring the current through the readout SQUIDS, while maintaining at high bandwidth the pure voltage bias needed for the phonon sensors.

An alternative scheme [19, 20] is to interleave the ionization electrodes and the phonon collectors on both detector faces. On one face the ionization electrodes are at positive voltage and connected to one amplifier, while on the other face they are at negative voltage and connected to a second amplifier. The phonon sensors remain at ground on both faces. In this arrangement, the electric field close to the surfaces is roughly parallel to the detector face and so a surface interaction generates a signal in the near-side charge amplifier only. Bulk events experience a field perpendicular to the faces, causing the electrons and holes from an event to generate equal signals in each charge amplifier. The interleaved design thus provides an additional means of discriminating surface events from bulk events.

Since the interleaved phonon sensors on both sides of the crystal remain at ground for the ionization measurement, the biasing electronics remain unchanged from the present implementation. If the surface identification works at the outer edges of the detector, no outer guard electrode is needed, and the readout and electronics of the two ionization channels also remain unchanged from the the present ZIP implementation of CDMS II.

4 Improving Manufacturability

At the CDMS II detector production rate of about one detector per month, or 3 kg Ge per year, deploying a ton of detectors would be impossible. Fortunately, nearly all the time associated with detector production is spent on a lengthy program of testing and repairing, which could be rendered unnecessary by improvements to the fabrication process. These improvements would allow orders of magnitude increases in detector production. Furthermore, many of these fabrication improvements also allow easier building of the experimental infrastructure and decrease the cryostat's material and heatload.

Several straightforward improvements are planned to increase fabrication yield. Changing to a whole-field mask for first-layer exposures, optimizing etching recipes, and switching from $1\ \mu\text{m}$ to $2\ \mu\text{m}$ features should greatly reduce photolithography errors and the resulting need for testing and repair. These changes should increase the fabrication rate by a factor of 5.

Further increases require reducing or eliminating the need for cryogenic testing of the W thin-film critical temperature. The addition of a mechanical planetary system for W film depositions may result in reproducible, uniform critical temperatures. The sensitivity of W to processing conditions has, in addition, motivated work to develop alternative films such as Al(Mn) that may be more reproducibly processed [21]. Finally, studying W film properties (crystalline phase, resistivity, film thickness, crystallite size and sputtering conditions) may lead to the establishment of room-temperature diagnostic tests.

4.1 Lower-Inductance SQUID Readout

In CDMSII the transition-edge sensors (TESs) of each phonon sensor are in series with the input coil to a SQUID array of 100 elements. A voltage is applied across the combined TES/input coil pair, and the SQUID array output measures the current through the TES. In order to have sensitivity to resolve the TES current of phonon events, the SQUID array must have many turns on the input coil for flux amplification. However, the ratio of the input inductance of the SQUID array to the operating dynamic resistance of the TES, $L_{\text{in}}(\text{array})/R_{\text{dyn}}(\text{TES})$, sets a limit on bandwidth. For the phonon sensor readout to have sufficient bandwidth ($\sim 100\ \text{kHz}$) and to be stable from electrothermal oscillations, the dynamic resistance of the phonon sensor $R_{\text{dyn}} > 0.1\ \Omega$.

A number of the proposed advances of our phonon sensor technology described above would benefit from a decrease of L_{in} . These include the increase of the coverage of the phonon sensors, which would require connecting more TESs in parallel; the widening of the W TES to ease the fabrication; and the use of Al(Mn), which has intrinsically lower resistivity. Moreover, the phonon rejection would likely benefit from the increased speed.

Two approaches are possible. One is to decrease the apparent input inductance through feedback. Replacing our current magnetic feedback through a feedback coil with a resistive feedback to the input of the SQUID would decrease the effective inductance by the gain of the feedback loop. This scheme requires no modification of the warm electronics and only a minor rewiring on the cold electronics stage.

A second approach is to use a single SQUID front end, so that the input inductance is physically smaller. This scheme requires a two-stage SQUID configuration, such as has been operated for many years [22]. A voltage-biased single SQUID is the initial sensor of TES current. The current from the single SQUID is amplified by a second-stage SQUID array similar to the single-stage

array used in CDMS II. A two-stage system has greater current sensitivity at the first-stage input and hence greater signal to noise. The two-stage system also imposes less stringent design and fabrication requirements on the SQUID array. With a first-stage preamplifier SQUID, less gain is required in the SQUID array; the fewer turns on the input coil result in greater reliability in the SQUID fabrication and operation.

4.2 SQUID Ionization Readout

Schemes using SQUID amplifiers to read out the ionization channels would eliminate the need for tensioned signal wires going inside vacuum coax from 50 mK to 4 K, thus allowing the bulky, massive mounting hardware to be made much lighter and more flexible. Using SQUIDS would also decrease radically the power dissipated, an important consideration given the number of channels needed for SuperCDMS.

To provide enough sensitivity to measure the ionization current with SQUIDS, a high turn-ratio superconducting transformer (1:2000) would be coupled to a two-stage SQUID. The challenges of controlling stray capacitance and internal resonance for such a large transformer appear manageable, and performance at least as good as that of CDMS appears achievable [23]. This approach uses the same type of amplifier as the phonon sensors, thus simplifying the overall electronics systems.

5 Conclusions

Modest improvements in the level and/or discrimination of backgrounds are needed to keep backgrounds negligible during the three phases of SuperCDMS. By developing production designs that require only modest testing, detector production rates may be improved sufficiently to allow an exposure of 500 ton d within a reasonable time and budget. Overall, the improvement estimates described above are conservative. Previous development efforts have shown that some areas prove easier and provide larger factors while others prove more difficult. The conservative estimates together with the broad approach reduce the risk and give us confidence that we will succeed, providing the surest way to probe to WIMP-nucleon cross sections of 10^{-46} cm².

References

1. B. W. Lee and S. Weinberg. *Phys. Rev. Lett.*, **39**, 165 (1977).
2. J. R. Primack, D. Seckel, and B. Sadoulet. *Annu. Rev. Nucl. Part. Sci.*, **38**, 751 (1988).
3. L. Bergstrom. *Rep. Prog. Phys.*, **63**, 793 (2000).
4. J. D. Lewin and P. F. Smith. *Astropart. Phys.*, **6**, 87 (1996).

5. G. Jungman, M. Kamionkowski, and K. Griest. *Phys. Rep.* **267**, 195 (1996); J. Ellis, T. Falk, K. A. Olive, and M. Schmitt. *Phys. Lett.* **B413**, 355 (1997).
6. D.S. Akerib et al (CDMS Collaboration), these proceedings.
7. Y.G. Kim et al, *J. High Energy Phys.* **0212**, 034 (2002)
8. G.F. Giudice and A. Romanino, *Nucl. Phys. B* **699**, 65 (2004).
9. A. Pierce, *Phys. Rev.*, **D70**, 075006 (2004).
10. E.A. Baltz and P. Gondolo, *J. High Energy Phys.* **0410**, 052 (2004).
11. M. Battaglia et al, *Eur. Phys. J.* **C33**, 273 (2004).
12. K.D. Irwin et al, *Rev. Sci. Instr.* **66**, 5322 (1995); R.M. Clarke et al, In: *Proceedings of the Second International Workshop on the Identification of Dark Matter*, ed by N.J.C. Spooner and V. Kudryavtsev (World Scientific, Singapore, 1999), pp 353–358; T. Saab et al, *AIP Proc.* **605**, 497 (2002).
13. T. Shutt et al, *Nucl. Instr. Meth. A* **444**, 340 (2000).
14. R.M. Clarke et al, *Appl. Phys. Lett.* **76**, 2958 (2000).
15. V. Mandic et al, *Nucl. Instr. Meth. A* **520**, 171 (2004).
16. R. J. Gaitskell, in: N. J. C. Spooner, V. Kudryavtsev (Eds.), *Proceedings of the Third International Workshop on the Identification of Dark Matter*, World Scientific, London, 2001, pp. 606–617.
17. R. W. Schnee, D. S. Akerib, and R.J. Gaitskell, *Nucl. Phys. B (Proc. Suppl.)* **124**, 233 (2003).
18. D. Abrams et al (CDMS Collaboration), *Phys. Rev.* **D66**, 122003 (2002).
19. P. Luke, *Appl. Phys. Lett.* **65**(22):2884 (1994).
20. B. Cabrera, et al, in preparation.
21. B.A. Young et al, *Nucl. Instrum. and Meth. in Phys. Res.* **A520**, 307 (2004); S.W. Deiker et al, *Appl. Phys. Lett.* **85**, 2137 (2004).
22. K. D. Irwin et al, *Nucl. Instr. and Meth. in Phys. Res.* **A444**, 184 (2000).
23. K. D. Irwin et al, in preparation.